



HAL
open science

Communication-less Aerial Co-Manipulation with Cables and the Fundamental role of Internal Force

Marco Tognon, Chiara Gabellieri, Lucia Pallottino, Antonio Franchi

► **To cite this version:**

Marco Tognon, Chiara Gabellieri, Lucia Pallottino, Antonio Franchi. Communication-less Aerial Co-Manipulation with Cables and the Fundamental role of Internal Force. 2017. hal-01551105v2

HAL Id: hal-01551105

<https://laas.hal.science/hal-01551105v2>

Preprint submitted on 19 Sep 2017 (v2), last revised 11 Feb 2018 (v3)

HAL is a multi-disciplinary open access archive for the deposit and dissemination of scientific research documents, whether they are published or not. The documents may come from teaching and research institutions in France or abroad, or from public or private research centers.

L'archive ouverte pluridisciplinaire **HAL**, est destinée au dépôt et à la diffusion de documents scientifiques de niveau recherche, publiés ou non, émanant des établissements d'enseignement et de recherche français ou étrangers, des laboratoires publics ou privés.

Communication-less Aerial Co-Manipulation with Cables and the Fundamental role of Internal Force

Marco Tognon¹, Chiara Gabellieri^{1†}, Lucia Pallottino², and Antonio Franchi¹

Abstract—This paper considers the study of cooperative manipulation of a cable-suspended load with two aerial robots and without explicit communication. The role of the internal force for the asymptotic stability of the beam-position/beam-attitude equilibria is analyzed in depth. Using a nonlinear Lyapunov-based approach, we prove that if a non-zero internal force is chosen then asymptotic stabilization of any desired beam-pose configuration can be achieved with a decentralized and communication-less master-slave admittance controller. If, conversely, a zero internal force is chosen, as done in the majority of the state-of-the-art algorithms, the attitude of the beam is not controllable without communication. Non-zero internal force can be interpreted then as a fundamental factor that enables the use of cables as implicit communication means between the two aerial vehicles in replacement of the explicit ones. Furthermore, the formal proof of the system output-strictly passivity with respect to an energy-like storage function and a certain input-output pair is given. This proves the stability and the robustness of the method even during motion. The theoretical findings are validated through numerical simulations with added noise and realistic uncertainty.

I. INTRODUCTION

Over the last decade UAVs (Unmanned Aerial Vehicles) have risen the interest of a larger and larger audience for their wide application domain. Recently, aerial physical interaction, using aerial manipulators [1], [2] or exploiting physical links as cables [3], has become a very popular topic. One very interesting and applicative problem is the aerial manipulation of large objects. A cooperative approach allows to overcome the limited payload problem, thus lifting larger and heavier loads [4].

Many works targeted this problem proposing different methods and solutions. In [5], [6] cooperative aerial transportation of a rigid and an elastic object is considered, respectively. In [7] the use of a robotic arm is exploited to address the problem. Aerial manipulation via cables is another interesting solution to the problem since it reduces the couplings between the load and the robot attitude dynamics. Examples of cooperative aerial manipulation using cables are studied in [8]–[10]. All these examples rely on a centralized and model-based control strategy. Instead, a decentralized

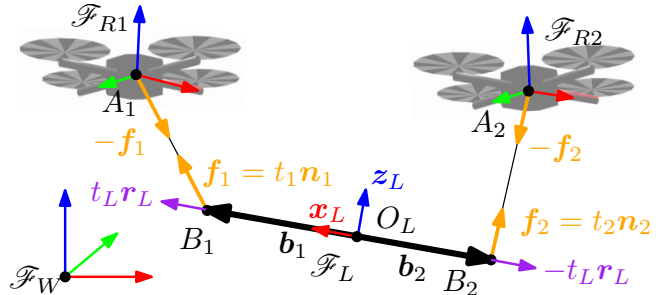


Fig. 1: Representation of the system and its major variables.

algorithm, as in [11], is more robust and scalable w.r.t. the number of robots.

However, the major bottleneck in decentralized algorithms is explicit communication. Communication delays and packet loss can affect the performance and even the stability of the systems. Limiting the need for explicit communication allows to reduce the complexity and to make the algorithm more scalable. In [12] the authors proposed one of the first decentralized leader-follower algorithm without explicit communication, for objects transportation performed by mobile ground robots. Aerial cooperative transportation by two robots without explicit communication has been addressed also in [13] for a cable-suspended beam-like load, and a leader-follower paradigm has been proposed. Here the leader follows an external position reference, while the horizontal position of the follower is controlled with an admittance filter, trying to keep the cable always vertical (zero internal force). A similar approach has been proposed in [14] but relying on a visual feedback. However, those methods do not deal with the load pose control and do not provide a formal stability proof.

For the same system composed by two aerial robots carrying a cable suspended beam-like load (see Fig. 1 for a schematic representation), we propose a decentralized algorithm relying only on implicit communication. Our algorithm uses a master-slave architecture, where both robots are controlled with an admittance filter (not only the slave as in the related state of the art), to make the overall system more compliant to external disturbances. One of our main contributions is the constructive and intuitive method to choose the controller input to stabilize the load in a desired pose (both position and orientation). the control of both turns the simpler transportation task found in the state of the art in a full-manipulation one. We show that those constant inputs are parametrized by the internal force of the load that plays

[†]The first two authors have equally collaborated to the manuscript, and can both be considered as first author.

¹LAAS-CNRS, Université de Toulouse, CNRS, Toulouse, France, antonio.franchi@laas.fr, marco.tognon@laas.fr, cgabellieri@laas.fr

²Centro di ricerca E. Piaggio, Università di Pisa, Largo Lucio Lazzarino 1, 56122, Pisa, Italy lucia.pallottino@unipi.it

This work has been funded by the European Union's Horizon 2020 research and innovation program under grant agreement No 644271 AEROARMS.

a crucial role on the equilibria stability. In particular, we prove that it has to be non-zero if one wants to stabilize the load at a certain desired pose. Differently from the state of the art algorithms, which are not formally guaranteed to converge, we instead also provide a formal proof of the stability through Lyapunov's direct method. Furthermore, we prove that the controlled system is output-strictly passive w.r.t. the relevant input-output pair. This provides a bound for the energy variations during the manipulation and an index of robustness of the method.

The paper is organized as follows: In Sec. II we derive the model. In Sec. III we present the control strategy and the equilibria of the system. Their stability is discussed in Sec. IV. In Sec. V we prove the passivity and stability of transportation. Simulation results and conclusive discussions are presented in Sec. VI and VII, respectively.

II. SYSTEM MODELING

The considered system and its major variables are shown in Fig. 1. The beam-like *load* to be manipulated is modeled as a rigid body with mass $m_L \in \mathbb{R}_{>0}$ and a positive definite inertia matrix $\mathbf{J}_L \in \mathbb{R}^{3 \times 3}$. We define the frame $\mathcal{F}_L = \{O_L, \mathbf{x}_L, \mathbf{y}_L, \mathbf{z}_L\}$ rigidly attached to the load, where O_L is the load center of mass (CoM). Furthermore, we define an inertial frame $\mathcal{F}_W = \{O_W, \mathbf{x}_W, \mathbf{y}_W, \mathbf{z}_W\}$ with \mathbf{z}_W oriented in the opposite direction to the gravity vector. The configuration of the load is then described by the position and orientation of \mathcal{F}_L with respect to \mathcal{F}_W , i.e., by the vector ${}^W\mathbf{p}_L \in \mathbb{R}^3$ and the rotation matrix ${}^W\mathbf{R}_L \in SO(3)$, respectively¹. Its dynamics is given by the Newton-Euler equations

$$\begin{aligned} m_L \ddot{\mathbf{p}}_L &= -m_L g \mathbf{e}_3 + \mathbf{f}_e \\ \dot{\mathbf{R}}_L &= \mathbf{S}(\boldsymbol{\omega}_L) \mathbf{R}_L \\ \mathbf{J}_L \dot{\boldsymbol{\omega}}_L &= -\mathbf{S}(\boldsymbol{\omega}_L) \mathbf{J}_L \boldsymbol{\omega}_L + \boldsymbol{\tau}_e - \boldsymbol{\omega}_L^\top \mathbf{B}_L \boldsymbol{\omega}_L, \end{aligned}$$

where, $\boldsymbol{\omega}_L \in \mathbb{R}^3$ is the angular velocity of \mathcal{F}_L w.r.t. \mathcal{F}_W expressed in \mathcal{F}_L , $\mathbf{S}(\star)$ is the operator such that $\mathbf{S}(\mathbf{x})\mathbf{y} = \mathbf{x} \times \mathbf{y}$, g is the gravitational constant, \mathbf{e}_i is the canonical unit vector with a 1 in the i -th entry, \mathbf{f}_e and $\boldsymbol{\tau}_e \in \mathbb{R}^3$ are the sum of external forces and moments acting on the load, respectively. The positive definite matrix $\mathbf{B}_L \in \mathbb{R}^{3 \times 3}$ is a damping factor modeling the energy dissipation phenomena.

The load is transported by two aerial robots by means of two cables, one for each robot. We denote with A_i the attachment point of the i -th cable to the i -th robot, with $i = 1, 2$, and we define the frame $\mathcal{F}_{Ri} = \{A_i, \mathbf{x}_{Ri}, \mathbf{y}_{Ri}, \mathbf{z}_{Ri}\}$ rigidly attached to the robot and centered in the attachment point. The i -th robot configuration is described by the position and orientation of \mathcal{F}_{Ri} with respect to \mathcal{F}_W , denoted by the vector $\mathbf{p}_{Ri} \in \mathbb{R}^3$, and the rotation matrix $\mathbf{R}_{Ri} \in SO(3)$, respectively. We assume that the aerial robot can track any C^2 trajectory with negligible error in the domain of interest, independently from external disturbances. Indeed, with the recent robust controllers and disturbance observers for aerial vehicles, one can obtain very precise motions, even in the presence of

external disturbances. Moreover, if the used robot has a multi-directional thrust, as, e.g., the one presented in [15], then this assumption is exactly met thanks to its ability to compensate any external force almost instantaneously. The closed loop translational dynamics of the robot subjected to the position controller is then assumed as the one of a double integrator: $\ddot{\mathbf{p}}_{Ri} = \mathbf{u}_{Ri}$, where \mathbf{u}_{Ri} is a virtual input to be designed. At this stage it might seem that we are assuming a controller and an actuation system that can make the platform 'infinitely stiff' w.r.t. the force produced by the cable. However, we shall re-introduce a compliant behavior by suitably designing the input \mathbf{u}_{Ri} to safely react to the force produced by the cable on the robot. This is a common paradigm in interaction control.

The other end of the i -th cable is attached to the load at the anchoring point B_i described by the vector ${}^L\mathbf{b}_i \in \mathbb{R}^3$ denoting its position with respect to \mathcal{F}_L . The position of B_i in \mathcal{F}_W is then given by $\mathbf{b}_i = \mathbf{p}_L + \mathbf{R}_L {}^L\mathbf{b}_i$.

Assumption 1. The two anchoring points are placed such that the load CoM coincides with their middle point, i.e., ${}^L\mathbf{b}_1 = -{}^L\mathbf{b}_2$. This assumption is rather easy to meet in practice, even for a load with non uniformly distributed mass.

To simplify the discussion we assume, without loss of generality, that \mathbf{x}_L is aligned with the line passing through B_1 and B_2 and pointing toward B_1 . It results ${}^L\mathbf{b}_1 = [\|{}^L\mathbf{b}_1\| \ 0 \ 0]^\top$.

We model the i -th cable as a unilateral spring along its principal direction, characterized by a constant elastic coefficient $k_i \in \mathbb{R}_{>0}$, a constant nominal length denoted by l_{0i} and a negligible mass and inertia w.r.t. the ones of the robots and of the load. The attitude of the cable is described by the normalized vector, $\mathbf{n}_i = \mathbf{l}_i / \|\mathbf{l}_i\|$, where $\mathbf{l}_i = \mathbf{p}_{Ri} - \mathbf{b}_i$. Given a certain elongation $\|\mathbf{l}_i\|$ of the cable, the latter produces a force acting on the load at B_i equal to:

$$\mathbf{f}_i = t_i \mathbf{n}_i, \quad t_i = \begin{cases} k_i (\|\mathbf{l}_i\| - l_{0i}) & \text{if } \|\mathbf{l}_i\| - l_{0i} > 0 \\ 0 & \text{otherwise} \end{cases}. \quad (1)$$

$t_i \in \mathbb{R}_{\geq 0}$ denotes the tension along the cable and it is given by the simplified Hooke's law. When the tension is zero the cable is considered slack. However, as usually done in the related literature, we assume that the controller and the gravity force always maintain the cables taut, at least in the domain of interest². The force produced at the other hand of the cable, namely on the i -th robot at A_i , is equal to $-\mathbf{f}_i$.

Considering the forces that robots and load exchange by means of the cables, the dynamics of the full system is:

$$\begin{aligned} \dot{\mathbf{v}}_R &= \mathbf{u}_R \\ \dot{\mathbf{v}}_L &= \mathbf{M}_L^{-1} (-\mathbf{c}_L(\mathbf{v}_L) - \mathbf{g}_L + \mathbf{G}(\mathbf{q}_L) \mathbf{f}), \end{aligned} \quad (2)$$

where $\mathbf{q}_R = [\mathbf{p}_{R1}^\top \ \mathbf{p}_{R2}^\top]^\top$, $\mathbf{q}_L = (\mathbf{p}_L, \mathbf{R}_L)$, $\mathbf{v}_R = [\dot{\mathbf{p}}_{R1}^\top \ \dot{\mathbf{p}}_{R2}^\top]^\top$, $\mathbf{v}_L = [\dot{\mathbf{p}}_L^\top \ \boldsymbol{\omega}_L^\top]^\top$, $\mathbf{u}_R = [\mathbf{u}_{R1}^\top \ \mathbf{u}_{R2}^\top]^\top$, $\mathbf{f} = [\mathbf{f}_1^\top \ \mathbf{f}_2^\top]^\top$ where \mathbf{f}_i is given in (1), and is a function of the state, $\mathbf{M}_L =$

¹The left superscript indicates the reference frame. From now on, \mathcal{F}_W is considered as reference frame when the superscript is omitted.

²We are not interested here in 'fancy' acrobatic motions of the load but rather on designing a decentralized and communicationless control law that can be employed in realistic scenarios.

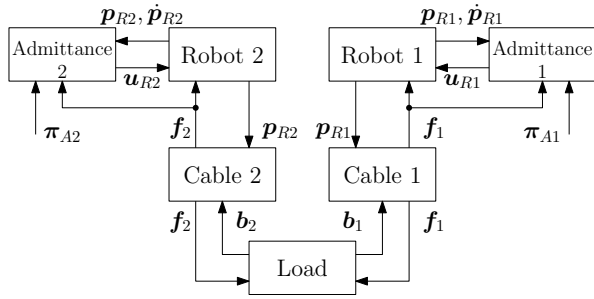


Fig. 2: Schematic representation of the overall system including both physical and control blocks.

$\text{diag}(m_L \mathbf{I}_3, \mathbf{J}_L)$ and $\mathbf{I}_3 \in \mathbb{R}^{3 \times 3}$ the identity matrix, $\mathbf{g}_L = [-m_L g e_3^\top \mathbf{0}^\top]^\top$ and

$$\mathbf{c}_L = \begin{bmatrix} \mathbf{0} \\ \mathbf{S}(\boldsymbol{\omega}_L) \mathbf{J}_L \boldsymbol{\omega}_L \end{bmatrix} \quad \mathbf{G} = \begin{bmatrix} \mathbf{I}_3 & \mathbf{I}_3 \\ \mathbf{S}({}^L \mathbf{b}_1) \mathbf{R}_L^\top & \mathbf{S}({}^L \mathbf{b}_2) \mathbf{R}_L^\top \end{bmatrix}.$$

We remark that the two dynamics in (2) are coupled together by the cable forces in (1).

Control problem

In this work we aim to: i) stabilize the load at a desired configuration, $\bar{\mathbf{q}}_L = (\bar{\mathbf{p}}_L, \bar{\mathbf{R}}_L)$; ii) preserve the stability of the load during its transportation.

Assuming a perfect knowledge of the system dynamic model, and a perfect state estimation, one could use a centralized control approach, as in [8], [9]. We are instead interested in solving the mentioned objectives using a decentralized approach without explicit communication between robots and relying on a minimal sensorial setup.

III. CONTROL DESIGN AND EQUILIBRIA

To achieve the control objectives of Sec. II we propose the use of an admittance filter for *both* robots, i.e., setting:

$$\mathbf{u}_{Ri} = \mathbf{M}_{Ai}^{-1} (-\mathbf{B}_{Ai} \dot{\mathbf{p}}_{Ri} - \mathbf{K}_{Ai} \mathbf{p}_{Ri} - \mathbf{f}_i + \boldsymbol{\pi}_{Ai}), \quad (3)$$

where the three positive definite matrices $\mathbf{M}_{Ai}, \mathbf{B}_{Ai}, \mathbf{K}_{Ai} \in \mathbb{R}^{3 \times 3}$ are the virtual inertia of the robot, the virtual damping, and the stiffness of a virtual spring attached to the robot, and $\boldsymbol{\pi}_{Ai} \in \mathbb{R}^3$ is an additional input. Notice that (3) does not require explicit communication because it requires only local information, i.e., the state of the robot $(\mathbf{p}_{Ri}, \dot{\mathbf{p}}_{Ri})$, and the force applied by the cable \mathbf{f}_i . The first can be retrieved with standard on-board sensors for aerial vehicles, while the second can be directly measured by an on-board force sensor or estimated by a model-based observer as done in [13], [15]. The control strategy is schematically represented in Fig. 2.

Combining equations (2) and (3) we can write the closed loop system dynamics as

$$\dot{\mathbf{v}} = m(\mathbf{q}, \mathbf{v}, \boldsymbol{\pi}_A) = \begin{bmatrix} \mathbf{M}_A^{-1} (-\mathbf{B}_A \dot{\mathbf{p}}_R - \mathbf{K}_A \mathbf{p}_R - \mathbf{f} + \boldsymbol{\pi}_A) \\ \mathbf{M}_L^{-1} (-\mathbf{c}_L(\mathbf{v}_L) - \mathbf{g}_L + \mathbf{G}\mathbf{f}) \end{bmatrix} \quad (4)$$

with $\mathbf{q} = (\mathbf{q}_R, \mathbf{q}_L)$, $\mathbf{v} = [\mathbf{v}_R^\top \mathbf{v}_L^\top]^\top$ and $\boldsymbol{\pi}_A = [\boldsymbol{\pi}_{A1}^\top \boldsymbol{\pi}_{A2}^\top]^\top$. Furthermore $\mathbf{M}_A = \text{diag}(\mathbf{M}_{A1}, \mathbf{M}_{A2})$, $\mathbf{B}_A = \text{diag}(\mathbf{B}_{A1}, \mathbf{B}_{A2})$ and $\mathbf{K}_A = \text{diag}(\mathbf{K}_{A1}, \mathbf{K}_{A2})$.

In order to coordinate the motions of the robots in a decentralized way we propose a master-slave approach. In this way only one robot, namely the designated master, will have an active control of the system. Choosing robot 1 as master and robot 2 as slave we simply set $\mathbf{K}_{A1} \neq \mathbf{0}$, $\mathbf{K}_{A2} = \mathbf{0}$ to obtain the sought master-slave paradigm.

We say that \mathbf{q} is an *equilibrium configuration* if $\exists \boldsymbol{\pi}_A$ s.t. $\mathbf{0} = m(\mathbf{q}, \mathbf{0}, \boldsymbol{\pi}_A)$, i.e. if the corresponding zero-velocity state $(\mathbf{q}, \mathbf{0})$ is a forced equilibrium for the system (4) for a certain forcing input $\boldsymbol{\pi}_A$. We say that an equilibrium configuration \mathbf{q} is stable, unstable, or asymptotically stable if $(\mathbf{q}, \mathbf{0})$ is stable, unstable, or asymptotically stable, respectively.

In the following we shall prove that for any desired load configuration $\bar{\mathbf{q}}_L$ there exists a set $\Pi_A(\bar{\mathbf{q}}_L) \subset \mathbb{R}^6$ such that for any $\boldsymbol{\pi}_A \in \Pi_A(\bar{\mathbf{q}}_L)$ one can compute a $\bar{\mathbf{q}}_R$, depending on $\bar{\mathbf{q}}_L$ and $\boldsymbol{\pi}_A$, that makes $\bar{\mathbf{q}} = (\bar{\mathbf{q}}_L, \bar{\mathbf{q}}_R)$ an asymptotically stable equilibrium with $\boldsymbol{\pi}_A$ as forcing input. Furthermore, we shall also give the analytic expression of $\Pi_A(\bar{\mathbf{q}}_L)$ and the fundamental guidelines on how to choose $\boldsymbol{\pi}_A \in \Pi_A(\bar{\mathbf{q}}_L)$.

As we shall see, a key role in all the following analyses is played by the *load internal force*, defined as

$$t_L := \frac{1}{2} \mathbf{f}^\top \begin{bmatrix} \mathbf{I}_3 \\ -\mathbf{I}_3 \end{bmatrix} \mathbf{R}_L e_1 =: \frac{1}{2} \mathbf{f}^\top \mathbf{r}_L. \quad (5)$$

For the particular choice of \mathbf{r}_L , we have that if $t_L > 0$ the internal force is a *tension* (the work of the internal force is positive if the distance between the anchoring points increases) while if $t_L < 0$ the internal force is a *compression* (viceversa, the work is positive if the distance decreases).

A. Equilibrium Configurations of the Closed Loop System

We firstly carefully analyze and characterize the relation between equilibrium configurations, from now on simply called *equilibria*, and the forcing input $\boldsymbol{\pi}_A$. In particular, in the following we study:

- which is the *set of inputs* (and corresponding robot positions) that equilibrates a desired $\bar{\mathbf{q}}_L$ (theorem 1);
- which is the *set of equilibria* if the particular input chosen in the aforementioned set is applied on the system (theorem 2).

These two problems are referred to as the *equilibria direct problem* and *equilibria inverse problem*, respectively. A schematic representation of the results described in the theorems is given in Fig. 3.

Theorem 1 (equilibria direct problem). *Consider the closed loop system (4) and assume that the load is at a given desired configuration $\mathbf{q}_L = \bar{\mathbf{q}}_L = (\bar{\mathbf{p}}_L, \bar{\mathbf{R}}_L)$. For each internal force $t_L \in \mathbb{R}$, there exists a unique constant value for the forcing input $\boldsymbol{\pi}_A = \bar{\boldsymbol{\pi}}_A$ (and a unique position of the robots $\mathbf{q}_R = \bar{\mathbf{q}}_R$) such that $\bar{\mathbf{q}} = (\bar{\mathbf{q}}_L, \bar{\mathbf{q}}_R)$ is an equilibrium of the system.*

In particular $\bar{\boldsymbol{\pi}}_A$ and $\bar{\mathbf{q}}_R = [\bar{\mathbf{p}}_{R1}^\top \bar{\mathbf{p}}_{R2}^\top]^\top$ are given by

$$\bar{\boldsymbol{\pi}}_A(\bar{\mathbf{q}}_L, t_L) = \mathbf{K}_A \bar{\mathbf{q}}_R + \bar{\mathbf{f}}(\bar{\mathbf{q}}_L, t_L) \quad (6)$$

$$\bar{\mathbf{p}}_{Ri}(\bar{\mathbf{q}}_L, t_L) = \bar{\mathbf{p}}_L + \bar{\mathbf{R}}_L {}^L \mathbf{b}_i + \left(\frac{\|\bar{\mathbf{f}}_i\|}{k_i} + l_{0i} \right) \frac{\bar{\mathbf{f}}_i}{\|\bar{\mathbf{f}}_i\|}, \quad (7)$$

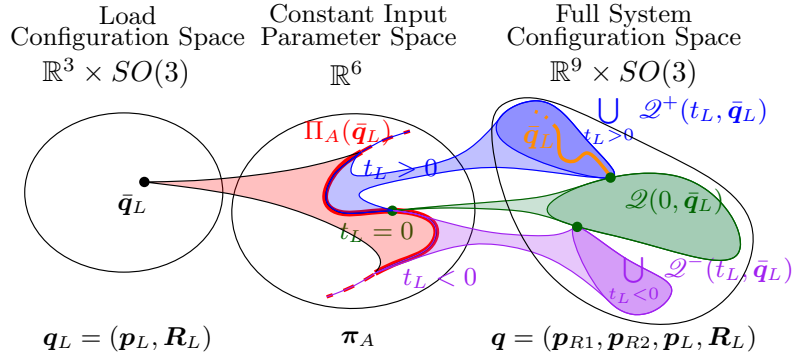


Fig. 3: Relation between the equilibria and forcing control input. In particular, starting from the left: to a desired load configuration of equilibrium it corresponds a forcing input in the subset $\Pi_A(\bar{q}_L)$ of dimension one (direct problem). Then, moving to the right: to a forcing input in $\Pi_A(\bar{q}_L)$ it corresponds an equilibrium in the subsets $\mathcal{Q}^+(t_L, \bar{q}_L)$, $\mathcal{Q}^-(t_L, \bar{q}_L)$ or $\mathcal{Q}(0, \bar{q}_L)$ according to the value of t_L (inverse problem). The orange line inside $\mathcal{Q}^+(t_L, \bar{q}_L)$ corresponds to the equilibria $\mathbf{q} \in \mathcal{Q}^+(t_L, \bar{q}_L)$ such that $\mathbf{q}_L = \bar{q}_L$.

for $i = 1, 2$, where

$$\bar{\mathbf{f}}(\bar{q}_L, t_L) = \begin{bmatrix} \bar{\mathbf{f}}_1 \\ \bar{\mathbf{f}}_2 \end{bmatrix} = \frac{m_L g}{2} \begin{bmatrix} \mathbf{I}_3 \\ \mathbf{I}_3 \end{bmatrix} \mathbf{e}_3 + t_L \begin{bmatrix} \mathbf{I}_3 \\ -\mathbf{I}_3 \end{bmatrix} \bar{\mathbf{R}}_L \mathbf{e}_1. \quad (8)$$

Proof. The desired load configuration \bar{q}_L can be equilibrated if there exists at least a \bar{q}_R and a π_A such that:

$$m(\bar{q}, \mathbf{0}, \pi_A) = \mathbf{0}. \quad (9)$$

Consider the last six rows of (9). We must find the \mathbf{f} resolving

$$\mathbf{G}\mathbf{f} = \mathbf{g}_L. \quad (10)$$

\mathbf{G} is not invertible since $\text{rank}(\mathbf{G}) = 5$, thus we have to verify that a solution for (10) exists. Expanding (10) we obtain

$$\mathbf{f}_1 + \mathbf{f}_2 = -m_L g \mathbf{e}_3 \quad (11)$$

$$\mathbf{S}(\mathbf{L}\mathbf{b}_1) \bar{\mathbf{R}}_L^\top \mathbf{f}_1 + \mathbf{S}(\mathbf{L}\mathbf{b}_2) \bar{\mathbf{R}}_L^\top \mathbf{f}_2 = \mathbf{0}. \quad (12)$$

Then, substituting in (12) the \mathbf{f}_1 obtained from (11) we have

$$2\mathbf{S}(\mathbf{L}\mathbf{b}_1) \bar{\mathbf{R}}_L^\top \mathbf{f}_2 = -\mathbf{S}(\mathbf{L}\mathbf{b}_1) \bar{\mathbf{R}}_L^\top m_L g \mathbf{e}_3, \quad (13)$$

for which $\mathbf{f}_2 = m_L g \mathbf{e}_3 / 2$ is always a solution. Therefore, all the solutions of (10) can be written as

$$\bar{\mathbf{f}} = \mathbf{G}^\dagger \mathbf{g}_L + \mathbf{r}_L t_L, \quad (14)$$

where $\mathbf{G}^\dagger = 1/2[\mathbf{I}_3 \ \mathbf{I}_3]^\top$ is the pseudo inverse of \mathbf{G} , $\mathbf{r}_L \in \mathbb{R}^6$ is a vector in $\ker(\mathbf{G})$, and $t_L \in \mathbb{R}$ is an arbitrary number. We computed \mathbf{r}_L from (11) and (12) putting the right hand side equal to zero, obtaining after some algebra $\mathbf{r}_L = [\mathbf{I}_3 \ -\mathbf{I}_3]^\top \bar{\mathbf{R}}_L \mathbf{e}_1$, as in the definition (5). Equation (14) can be then rewritten as (8). The expression of \bar{p}_{Ri} in (7) is computed using (1) and the kinematics of the system. Notice that (7) is singular when $\bar{\mathbf{f}}_i = \mathbf{0}$ for some i . However this can always be avoided properly choosing t_L .

Lastly, from the first six rows of (9) we have that \bar{q}_L is equilibrated if $\pi_A = \bar{\pi}_A$, where $\bar{\pi}_A$ is defined as in (6). \square

Remark 1. Based on Theorem 1 we can define a set $\Pi_A(\bar{q}_L) = \{\pi_A \in \mathbb{R}^6 : \pi_A = \bar{\pi}_A(\bar{q}_L, t_L) \text{ for } t_L \in \mathbb{R}\}$ which has dimension 1, since it is parametrized by the scalar $t_L \in \mathbb{R}$. This set is depicted as a curve in the middle set of Fig. 3.

Remark 2. Theorem 1 and its constructive proofs, give an intuitive method for choosing the forcing input π_A given a desired load configuration \bar{q}_L to equilibrate. In particular one has to choose only the value of the internal force t_L . We shall show that is always preferable to choose $t_L > 0$ to obtain an asymptotically stable equilibrium.

Once t_L is chosen and the input $\pi_A = \bar{\pi}_A(t_L, \bar{q}_L)$ is applied to the system, it is not in general granted that (\bar{q}_L, \bar{q}_R) is the only equilibrium of the closed loop system (4), i.e., contrary to the equilibria direct problem, the inverse one may have multiple solutions. The following results will show how many other equilibria exist and which is their nature.

Theorem 2 (equilibria inverse problem). *Given $t_L \in \mathbb{R}$ and the corresponding $\bar{\pi}_A \in \Pi_A(\bar{q}_L)$ computed as in (6), the equilibria of the system (4), when the input $\pi_A = \bar{\pi}_A(t_L, \bar{q}_L)$ is applied, are all and only the ones described by the following conditions*

$$\begin{aligned} t_L \bar{\mathbf{R}}_L \mathbf{e}_1 \times \bar{\mathbf{R}}_L \mathbf{e}_1 &= \mathbf{0} \\ \mathbf{p}_{R1} &= \bar{\mathbf{p}}_{R1} \\ \mathbf{p}_L &= \mathbf{p}_{R1} - \bar{\mathbf{R}}_L \mathbf{L} \mathbf{b}_1 - \left(\frac{\|\bar{\mathbf{f}}_1\|}{k_1} + l_{01} \right) \frac{\bar{\mathbf{f}}_1}{\|\bar{\mathbf{f}}_1\|} = \\ &= \bar{\mathbf{p}}_L + (\bar{\mathbf{R}}_L - \mathbf{R}_L) \mathbf{L} \mathbf{b}_1 \\ \mathbf{p}_{R2} &= \mathbf{p}_L + \mathbf{R}_L \mathbf{L} \mathbf{b}_2 + \left(\frac{\|\bar{\mathbf{f}}_2\|}{k_2} + l_{02} \right) \frac{\bar{\mathbf{f}}_2}{\|\bar{\mathbf{f}}_2\|}. \end{aligned} \quad (15)$$

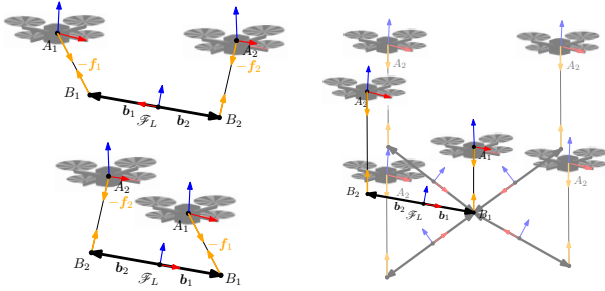
We denote with $\mathcal{Q}(t_L, \bar{q}_L)$ the set of configurations respecting (15).

Proof. Given $t_L \in \mathbb{R}$, and $\bar{\pi}_A \in \Pi_A(\bar{q}_L)$, a configuration \mathbf{q} is an equilibrium if $m(\mathbf{q}, \mathbf{0}, \bar{\pi}_A) = \mathbf{0}$. The first six rows are $\mathbf{K}_A \mathbf{q}_R + \mathbf{f} - \bar{\pi}_A = \mathbf{0}$. Then, from (6) we have that

$$\mathbf{f} = \mathbf{K}_A(\bar{q}_R - \mathbf{q}_R) + \bar{\mathbf{f}}. \quad (16)$$

Multiplying both sides of (16) by \mathbf{G} and using (10) we obtain $\mathbf{G}\mathbf{K}_A(\bar{q}_R - \mathbf{q}_R) + \mathbf{G}\bar{\mathbf{f}} = \mathbf{g}_L$. Then, using $\mathbf{K}_{A2} = \mathbf{0}$, and the expression of $\bar{\mathbf{f}}$ in (8), we get

$$\begin{bmatrix} \mathbf{K}_{A1} \mathbf{e}_{R1} \\ \mathbf{S}(\mathbf{L}\mathbf{b}_1) \bar{\mathbf{R}}_L \mathbf{K}_{A1} \mathbf{e}_{R1} \end{bmatrix} + \begin{bmatrix} m_L g \mathbf{e}_3 \\ 2\mathbf{S}(\mathbf{L}\mathbf{b}_2) \bar{\mathbf{R}}_L^\top \bar{\mathbf{R}}_L \mathbf{e}_1 t_L \end{bmatrix} = \begin{bmatrix} m_L g \mathbf{e}_3 \\ \mathbf{0} \end{bmatrix}, \quad (17)$$



(a) Two equilibria for $t_L \neq 0$. On the top and on the bottom one equilibrium configuration in $\mathcal{Q}^+(t_L, \bar{q}_L)$ and $\mathcal{Q}^-(t_L, \bar{q}_L)$, respectively. (b) Five of the infinite possible equilibria for $t_L = 0$. In vivid color the configuration \bar{q} . In opaque color some of the other possible equilibria in $\mathcal{Q}(0, \bar{q}_L)$.

Fig. 4: 2D representation of the equilibria varying t_L .

where $e_{Ri} = (\bar{p}_{Ri} - p_{Ri})$. The top row of (17) implies that $e_{R1} = 0$, hence $p_{R1} = \bar{p}_{R1}$. Replacing $e_{R1} = 0$ in the bottom part of (17) we obtain

$$\begin{aligned} S({}^L b_2) R_L^\top \bar{R}_L e_{1t_L} = 0 &\Leftrightarrow {}^L b_2 \times R_L^\top \bar{R}_L e_{1t_L} = 0 \\ &\Leftrightarrow R_L e_1 \times \bar{R}_L e_{1t_L} = 0. \end{aligned} \quad (18)$$

Finally we can retrieve the remaining components of the equilibrium configuration, namely p_L and p_{R2} , using (1) and the system kinematics. \square

Remark 3. If $t_L = 0$ the conditions in (18) hold for all possible load attitudes $R_L \in SO(3)$. This means that the set of equilibria with no internal force, i.e., $\mathcal{Q}(0, \bar{q}_L)$, contains all the $R_L \in SO(3)$ and the q_R, p_L are computed from R_L using (15). Figure 4b illustrates some of these equilibria.

For $t_L \neq 0$, it is required that $R_L e_1$ is parallel to $\bar{R}_L e_1$. This can be obtained with $R_L = R_L(k, \phi) = \bar{R}_L R_{z_L}(k\pi) R_{x_L}(\phi)$, where $k = 0, 1$, $\phi \in [0, 2\pi]$, and $R_{z_L}(\cdot)$ and $R_{x_L}(\cdot)$ are the rotations about z_L and x_L , respectively. Considering that ${}^L b_1$ is parallel to x_L we have that $R_{z_L}(k\pi) R_{x_L}(\phi) {}^L b_1$ is either equal to ${}^L b_1$ if $k = 0$ or to $-{}^L b_1$ if $k = 1$. Therefore, using (15), we obtain either $p_L = \bar{p}_L$ if $k = 0$ or $p_L = \bar{p}_L + 2R_L e_1$ if $k = 1$.

Fig. 4a provides a simplified representations of the two different sets of equilibria for $k = 0$ and $k = 1$, formally defined as follows:

- $\mathcal{Q}^+(t_L, \bar{q}_L) = \{q \in \mathcal{Q}(t_L, \bar{q}_L) | R_L = R_L(0, \phi) \forall \phi\}$,
- $\mathcal{Q}^-(t_L, \bar{q}_L) = \{q \in \mathcal{Q}(t_L, \bar{q}_L) | R_L = R_L(1, \phi) \forall \phi\}$.

Notice that $\mathcal{Q}(0, \bar{q}_L)$ is parametrized by an element in $SO(3)$ (any $R_L \in SO(3)$ is allowed), while $\mathcal{Q}^+(t_L, \bar{q}_L)$ and $\mathcal{Q}^-(t_L, \bar{q}_L)$, for $t_L \neq 0$, are parametrized by an element in $SO(1)$ ($R_L(0, \phi)$ and $R_L(1, \phi)$, for any $\phi \in [0, 2\pi]$, respectively). For all t_L , the load rotation about x_L is arbitrary. This because the robots can not apply any moment along x_L , and the corresponding rotation results uncontrollable. Practically this is not an issue since the orientation of a beam about x_L is usually not of interest and it is anyway passively stabilized by the structure.

At the end of this section we can conclude that choosing $t_L \neq 0$ (equilibrium with vertical cables) is the worse

option because every orientation of the load is contained in the equilibrium set for this choice. Furthermore, the load equilibrium positions are free to move on a sphere of radius $\|{}^L b_1\|$ centered on B_1 . Contrarily, $t_L \neq 0$ is a much better choice. In fact in this case, a part from the rotation about the x_L axis, there are only two distinct equilibria, and one it is exactly $q_L = \bar{q}_L$, as expected. For the other one the load orientation is parallel to the one in \bar{q}_L but its position is reflected w.r.t. B_1 (see Fig. 4a for an example).

IV. STABILITY OF THE EQUILIBRIA

In this section we shall analyze the stability of the equilibria discovered in Sec. III-A. Firstly we define $x = (q, v)$ as the state of the system, $\bar{x} = (\bar{q}, 0)$ the desired equilibrium state, and the following sets (subspaces of the state space) that are related to the previous sets of equilibria:

- $\mathcal{X}(t_L, \bar{q}_L) = \{x : q \in \mathcal{Q}(t_L, \bar{q}_L), v = 0\}$
- $\mathcal{X}(0, \bar{q}_L) = \{x : q \in \mathcal{Q}(0, \bar{q}_L), v = 0\}$
- $\mathcal{X}^+(t_L, \bar{q}_L) = \{x : q \in \mathcal{Q}^+(t_L, \bar{q}_L), v = 0\}$
- $\mathcal{X}^-(t_L, \bar{q}_L) = \{x : q \in \mathcal{Q}^-(t_L, \bar{q}_L), v = 0\}$

Theorem 3. *Let us consider a desired load configuration \bar{q}_L . For the system (4) let the constant forcing input π_A be chosen in $\Pi_A(\bar{q}_L)$ corresponding to a certain internal force t_L . Then x belonging to:*

- $\mathcal{X}^+(t_L, \bar{q}_L)$ is locally asymptotically stable if $t_L > 0$;
- $\mathcal{X}^-(t_L, \bar{q}_L)$ is unstable if $t_L > 0$;
- $\mathcal{X}(0, \bar{q}_L)$ is locally asymptotically stable;
- $\mathcal{X}^+(t_L, \bar{q}_L)$ is unstable if $t_L < 0$;
- $\mathcal{X}^-(t_L, \bar{q}_L)$ is locally asymptotically stable if $t_L < 0$.

Proof. Let us consider the following Lyapunov candidate:

$$\begin{aligned} V(x) = &\frac{1}{2}(v_R^\top M_A v_R + e_R^\top K_A e_R + v_L^\top M_L v_L + \\ &+ k_1(\|l_1\| - l_{01})^2 - l_1^\top \bar{f}_1 + k_2(\|l_2\| - l_{02})^2) + \\ &- l_2^\top \bar{f}_2 + t_L(1 - (\bar{R}_L e_1)^\top R_L e_1) + V_0, \end{aligned} \quad (19)$$

where $V_0 \in \mathbb{R}_{\geq 0}$. $V(x)$ is a lower bounded, continuously differentiable function in the domain of interest. In order to prove that $V(x)$ is lower bounded it is sufficient to show that the terms $k_i(\|l_i\| - l_{0i})^2 - l_i^\top \bar{f}_i$, for $i = 1, 2$, are lower bounded. All the others are clearly lower bounded. This can be demonstrated by defining $a = 2\bar{f}_i/k_i$ and observing that :

$$\begin{aligned} (\|l_i\| - l_{0i})^2 - a^\top l_i &= \|l_i\|^2 - 2\|l_i\|l_{0i} + l_{0i}^2 - a^\top l_i \\ &\geq \|l_i\|^2 - 2\|l_i\|l_{0i} - \|a\|\|l_i\| \\ &\geq \|l_i\|^2 - (2l_{0i} + \|a\|)\|l_i\|. \end{aligned}$$

Therefore (19) is lower bounded. If $t_L \geq 0$, we can choose the term V_0 such that $V(x) \geq 0$ and $V(\bar{x}) = 0$. Notice that $V(x)$ is only positive semi definite. Indeed, $V(x) = 0$ for all $x \in \mathcal{X}(0, \bar{q}_L)$ and $x \in \mathcal{X}^+(t_L, \bar{q}_L)$ for $t_L > 0$.

Let us now compute the time derivative of (19):

$$\begin{aligned} \dot{V}(x) = &v_R^\top M_A \dot{v}_R + v_L^\top M_L \dot{v}_L + e_R^\top K_A v_R + \\ &+ k_1(\|l_1\| - l_{01}) \frac{l_1^\top}{\|l_1\|} \dot{l}_1 + k_2(\|l_2\| - l_{02}) \frac{l_2^\top}{\|l_2\|} \dot{l}_2 + \\ &+ \bar{f}_1^\top \dot{l}_1 + \bar{f}_2^\top \dot{l}_2 - t_L e_1^\top \bar{R}_L^\top \dot{R}_L e_1. \end{aligned} \quad (20)$$

Replacing (4), (1) and (8) in (20) we obtain

$$\begin{aligned}\dot{V} &= \mathbf{v}_R^\top \mathbf{M}_A \dot{\mathbf{v}}_R + \mathbf{v}_L^\top \mathbf{M}_L \dot{\mathbf{v}}_L + \mathbf{e}_R^\top \mathbf{K}_A \mathbf{v}_R + \\ &+ (\mathbf{f}_1 - t_L \tilde{\mathbf{R}}_L \mathbf{e}_1 - m_L g \mathbf{e}_3 / 2)^\top (\dot{\mathbf{p}}_{R1} - \dot{\mathbf{p}}_L - \dot{\tilde{\mathbf{R}}}_L^L \mathbf{b}_1) + \\ &+ (\mathbf{f}_2 + t_L \tilde{\mathbf{R}}_L \mathbf{e}_1 - m_L g \mathbf{e}_3 / 2)^\top (\dot{\mathbf{p}}_{R2} - \dot{\mathbf{p}}_L - \dot{\tilde{\mathbf{R}}}_L^L \mathbf{b}_2) + \\ &- t_L \mathbf{e}_1^\top \tilde{\mathbf{R}}_L^\top \dot{\tilde{\mathbf{R}}}_L \mathbf{e}_1 \\ &= -\mathbf{v}_R^\top \mathbf{B}_A \mathbf{v}_R - \omega_L^\top \mathbf{B}_L \omega_L,\end{aligned}$$

that is clearly negative semidefinite. In particular $\dot{V}(\mathbf{x}) = 0$ for all $\mathbf{x} \in \mathcal{E}\{\mathbf{x} : \mathbf{v}_R = \mathbf{0}, \omega_L = \mathbf{0}\}$

Since $V(\mathbf{x})$ is only positive semidefinite, to prove the asymptotic stability we rely on the *LaSalle's invariance principle* [16]. Let us define a positively invariant set $\Omega_\alpha = \{\mathbf{x} : V(\mathbf{x}) \leq \alpha$ with $\alpha \in \mathbb{R}_{>0}\}$. By construction Ω_α is compact since (19) is radially unbounded and Ω_0 is compact ($\Omega_0 = \mathcal{X}(0, \bar{\mathbf{q}}_L)$ and $\Omega_0 = \mathcal{X}^+(t_L, \bar{\mathbf{q}}_L)$ for $t_L = 0$ and $t_L > 0$, respectively, are both compact sets). Then we need to find the largest invariant set \mathcal{M} in $\mathcal{E} = \{\mathbf{x} \in \Omega_\alpha \mid \dot{V}(\mathbf{x}) = 0\}$. A trajectory $\mathbf{x}(t)$ belongs identically to \mathcal{E} if

$$\dot{V}(\mathbf{x}(t)) \equiv 0 \Leftrightarrow \begin{cases} \mathbf{v}_R(t) \equiv \mathbf{0} \\ \omega_L(t) \equiv \mathbf{0} \end{cases} \Leftrightarrow m(\mathbf{q}(t), \mathbf{0}, \boldsymbol{\pi}_A) = 0$$

for all $t \in \mathbb{R}_{>0}$. Therefore \mathbf{x} has to be an equilibrium, and from Theorem 2 we have that $\dot{V}(\mathbf{x}(t)) \equiv 0 \Leftrightarrow \mathbf{x}(t) \in \mathcal{X}(t_L, \bar{\mathbf{q}}_L)$. Thus we obtain $\mathcal{M} = \Omega_\alpha \cap \mathcal{X}(t_L, \bar{\mathbf{q}}_L)$.

For $t_L > 0$, it is easy to see that for a sufficiently small α , $\mathcal{X}^+(t_L, \bar{\mathbf{q}}_L) \subseteq \Omega_\alpha$ but $\mathcal{X}^-(t_L, \bar{\mathbf{q}}_L) \cap \Omega_\alpha = \emptyset$. This because $V(\mathbf{x}) = 0$ for $\mathbf{x} \in \mathcal{X}^+(t_L, \bar{\mathbf{q}}_L)$, while $V(\mathbf{x}) > 0$ for $\mathbf{x} \in \mathcal{X}^-(t_L, \bar{\mathbf{q}}_L)$. This comes from the fact that in (19), for $\mathbf{x} \in \mathcal{X}^-(t_L, \bar{\mathbf{q}}_L)$, the term $t_L(1 - (\tilde{\mathbf{R}}_L \mathbf{e}_1)^\top \mathbf{R}_L \mathbf{e}_1) = 2t_L > 0$. Therefore $\mathcal{M} = \mathcal{X}^+(t_L, \bar{\mathbf{q}}_L)$. All conditions of LaSalle's principle are satisfied and $\mathcal{X}^+(t_L, \bar{\mathbf{q}}_L)$ is locally asymptotically stable.

On the other hand, for $t_L = 0$ we have that $\mathcal{X}(t_L, \bar{\mathbf{q}}_L) \subseteq \Omega_\alpha$ for every sufficiently small α . Therefore $\mathcal{M} = \mathcal{X}(t_L, \bar{\mathbf{q}}_L)$ and, as before, we can conclude that $\mathcal{X}(t_L, \bar{\mathbf{q}}_L)$ is locally asymptotically stable for the LaSalle's invariance principle.

Now, let us investigate the stability for $t_L < 0$. As before, with an opportune choice of V_0 , we have that $V(\mathbf{x}) = 0$ for $\mathbf{x} \in \mathcal{X}^+(t_L, \bar{\mathbf{q}}_L)$. However $\mathcal{X}^+(t_L, \bar{\mathbf{q}}_L)$ is a set of accumulation for the points where $V(\mathbf{x}) < 0$. Indeed, consider $\mathbf{v} = \mathbf{0}$, $\mathbf{p}_{R1} = \bar{\mathbf{p}}_{R1}$, \mathbf{R}_L such that $(\tilde{\mathbf{R}}_L \mathbf{e}_1)^\top \mathbf{R}_L \mathbf{e}_1 = 1 - \varepsilon$, with $\varepsilon > 0$ arbitrarily small, \mathbf{p}_L and \mathbf{p}_{R2} as in (15). Under this conditions, we have that $V(\mathbf{x}) = t_L(1 - (\tilde{\mathbf{R}}_L \mathbf{e}_1)^\top \mathbf{R}_L \mathbf{e}_1) = t_L \varepsilon < 0$. Then, $\dot{V}(\mathbf{x}) < 0$ in a neighborhood of $\mathcal{X}^+(t_L, \bar{\mathbf{q}}_L)$. All conditions of *Chetaev's theorem* [16] are satisfied, and we can conclude that $\mathcal{X}^+(t_L, \bar{\mathbf{q}}_L)$ is an unstable set.

Finally, to study the stability of $\mathcal{X}^-(t_L, \bar{\mathbf{q}}_L)$ for $t_L \neq 0$, let us consider a desired load configuration $\bar{\mathbf{q}}'_L = (\bar{\mathbf{p}}'_L, \bar{\mathbf{R}}'_L)$ such that $\bar{\mathbf{p}}'_L = \bar{\mathbf{p}}'_L + 2\tilde{\mathbf{R}}_L \mathbf{e}_1$ and $\bar{\mathbf{R}}'_L = \mathbf{R}_L(1, \phi)$ for a certain ϕ . Then we choose $\boldsymbol{\pi}'_A \in \Pi_A(\bar{\mathbf{q}}'_L)$ with $t'_L = -t_L$. For the reasoning in Sec. III-A, we have that $\mathcal{X}^+(t'_L, \bar{\mathbf{q}}'_L) = \mathcal{X}^-(t_L, \bar{\mathbf{q}}_L)$. Furthermore, for the previous results, if $t_L > 0$, $t'_L < 0$ and $\mathcal{X}^+(t'_L, \bar{\mathbf{q}}'_L)$ is unstable. Therefore, $\mathcal{X}^-(t_L, \bar{\mathbf{q}}_L)$ is unstable too. A similar reasoning can be done to prove that $\mathcal{X}^-(t_L, \bar{\mathbf{q}}_L)$ is locally asymptotically stable for $t_L < 0$. \square

V. PASSIVITY AND STABILITY OF MANIPULATION

Theorem 3 characterizes the stability of all the possible static equilibria given a certain constant forcing input. In particular, it shows that one has to choose $t_L > 0$ and $\boldsymbol{\pi}_A \in \Pi_A(\bar{\mathbf{q}}_L)$ to let the system asymptotically converge to a desired load configuration. On the contrary, one must avoid $t_L = 0$ because the control of the load attitude and its position is not possible. Notice that this last case is the most used in the literature, where the cables are tried to be kept always vertical, i.e., with no internal forces.

Let us now show how one can exploit the input $\boldsymbol{\pi}_{A1}$ in order to move the load between two distinct positions.

From (6)–(8) and from the fact that $\mathbf{K}_{A2} = \mathbf{0}$, it descends that only $\bar{\boldsymbol{\pi}}_{A1}$, in $\bar{\boldsymbol{\pi}}_A = [\bar{\boldsymbol{\pi}}_{A1}^\top \bar{\boldsymbol{\pi}}_{A2}^\top]^\top$, actually depends on the desired load position $\bar{\mathbf{p}}_L$. This makes robot 1 able to steer alone the load position without communicating with robot 2. This is implemented by first plugging a new desired position $\bar{\mathbf{p}}'_L$ in (6) thus computing a new $\bar{\mathbf{p}}'_{R1}$, and then plugging $\bar{\mathbf{p}}'_{R1}$ in (7) in order to compute the new constant forcing input $\bar{\boldsymbol{\pi}}'_{A1}$.

However, one may want to minimize the transient phases generated by a piecewise constant forcing input. It is sufficient to design $\boldsymbol{\pi}_{A1}$ as

$$\boldsymbol{\pi}_{A1}(t) = \bar{\boldsymbol{\pi}}_{A1} + \mathbf{u}_{A1}(t), \quad (21)$$

where $\mathbf{u}_{A1}(t)$ is a smooth function such that $\boldsymbol{\pi}_{A1}(0) = \bar{\boldsymbol{\pi}}_{A1}$ and $\boldsymbol{\pi}_{A1}(t_f) = \bar{\boldsymbol{\pi}}'_{A1}$ for $t_f \in \mathbb{R}_{>0}$. The smoothness of the whole maneuver can be adjusted by suitable tuning t_f and the smoothness of \mathbf{u}_{A1} . The same procedure can be repeated several times if the load position has to be steered across several via-points.

To formally ensure that the system remains stable when the input is time-varying, we shall prove that the system is output-strictly passive with respect to the input-output pair $(\mathbf{u}, \mathbf{y}) = (\mathbf{u}_A, \mathbf{v}_R)$.

Theorem 4. *If $\boldsymbol{\pi}_A$ is defined as in (21) for a certain $\bar{\mathbf{q}}$ and $\bar{\mathbf{q}}'$ with $t_L \geq 0$, then system (4) is output-strictly passive with respect to the storage function (19) and the input-output pair $(\mathbf{u}, \mathbf{y}) = (\mathbf{u}_A, \mathbf{v}_R)$.*

Proof. In the proof of theorem 3 we already shown that (19) is a continuously differentiable positive semidefinite function for $t_L \geq 0$, properly choosing V_0 . Furthermore, replacing (21) into (3), and differentiating (19) we obtain

$$\begin{aligned}\dot{V} &= -\mathbf{v}_R^\top \mathbf{B}_A \mathbf{v}_R + \mathbf{v}_R^\top \mathbf{u}_A - \omega_L^\top \mathbf{B}_L \omega_L \\ &\leq \mathbf{u}^\top \mathbf{y} - \mathbf{y}^\top \mathbf{B}_A \mathbf{y} = \mathbf{u}^\top \mathbf{y} - \mathbf{y}^\top \boldsymbol{\Phi}(\mathbf{y}),\end{aligned} \quad (22)$$

with $\mathbf{y}^\top \boldsymbol{\Phi}(\mathbf{y}) > 0 \forall \mathbf{y} \neq \mathbf{0}$. Therefore, system (4) is *output-strictly passive* [16]. \square

Thanks to the passivity of the system we can say that for a bounded input provided to the master, the energy of the system remains bounded too, and in particular it stabilizes to a new constant value as soon as \mathbf{u}_{A1} becomes constant again. This means that while moving the master, the overall state of the system will remain bounded, and will

converge to another specific equilibrium configuration when the master input becomes constant. Furthermore, it is well known that passivity is a robust property, especially with respect to model parameters. In other words, the system remains passive, and preserves all the nice stability properties, even changing the parameters of the system. In particular, choosing $\pi_A \in \Pi_A(\bar{q}_L)$ for a given \bar{q} , the system remains asymptotically stable even in the presence of some parameter uncertainties, but it will converge to a configuration that is slightly different from \bar{q} .

VI. NUMERICAL VALIDATION

In this section we shall describe the results of several numerical simulations validating the proposed method and all the presented theoretical concepts and results.

We tested the method in a more realistic scenario. Indeed, we replaced the simplified linear robot dynamics of Sec. II, with the proper nonlinear dynamics of a quadrotor-like vehicle together with a geometric position controller. All the system and control parameters are reported in Tab. I. Notice

System Parameters			Controller Gains		
	$i = 1$	$i = 2$		$i = 1$	$i = 2$
m_{Ri} [Kg]	1.02	0.993	M_{Ai}	$3\mathbf{I}_3$	$0.5\mathbf{I}_3$
\mathbf{J}_{Ri} [Kg · m ²]	$0.015\mathbf{I}_3$	$0.015\mathbf{I}_3$	\mathbf{B}_{Ai}	$18\mathbf{I}_3$	$1.3\mathbf{I}_3$
l_{0i} [m]	1	1	\mathbf{K}_{Ai}	$15\mathbf{I}_3$	$\mathbf{0}$
k_i [N/m]	20	20	Desired Load Pose		
${}^L\mathbf{b}_i$ [m]	$[0.433 \ 0 \ 0]$	$[-0.433 \ 0 \ 0]$	$\bar{\mathbf{p}}_L = [0.3 \ 0.3 \ 0.2]^T$ [m]		
$m_L = 0.900$ [Kg], $\mathbf{J}_{Lx} = 0.112$ [Kg · m ²]			$\bar{\phi} = 0$, $\bar{\theta} = \pi/8$ [rad]		
$\mathbf{J}_{Ly} = 5.681$, $\mathbf{J}_{Lz} = 5.681$ [Kg · m ²]			$\bar{\psi} = \pi/7$ [rad]		

TABLE I: Parameters used in the simulations.

the smaller apparent inertia of the slave, chosen to make it more sensitive to external forces, and thus more reactive.

Let us consider the desired equilibrium $\bar{q} = (\bar{\mathbf{p}}_L, \bar{\mathbf{R}}_L)$, whose value are in Tab. I, where $(\bar{\phi}, \bar{\theta}, \bar{\psi})$ are the Euler angles that parametrize $\bar{\mathbf{R}}_L$. We performed several simulations with $\pi_A \in \Pi_A(\bar{q}_L)$ computed as in (6) for the cases 1) $t_{L1} = 1.5$ [N] > 0, 2) $t_{L2} = 0$ [N], 3) $t_{L3} = -1$ [N] < 0,

To test the stability of the equilibria, we first initialized the system in different initial configurations and let it evolve. Figure 6 shows the position and orientation error for the three t_L and several different initial conditions. We have found what follows:

- 1) For $t_L = t_{L1}$, the system always converges to a state belonging to $\mathcal{X}^+(t_L, \bar{q}_L)$, independently from the initial state, validating the asymptotic stability of $\mathcal{X}^+(t_L, \bar{q}_L)$ when $t_L > 0$. In Fig. 5a we show the evolution of the system starting from two different initial states.
- 2) For t_{L2} , the system final state belongs to $\mathcal{X}(0, \bar{q}_L)$. The final attitude of the load depends on the initial state. In Fig. 5b we show the evolution of the system starting from two different initial states.
- 3) For t_{L3} , the system never converges to $\mathcal{X}^+(t_L, \bar{q}_L)$ even initializing it very close. This is due to the instability of $\mathcal{X}^+(t_L, \bar{q}_L)$ when $t_L < 0$. Figure 5b shows this result.

In another set of simulations, the master input $\pi_{A1}(t)$ is chosen as in (21) to bring the load in $\bar{\mathbf{p}}'_L = [4.5 \ 4.5 \ 5]^T$ [m].

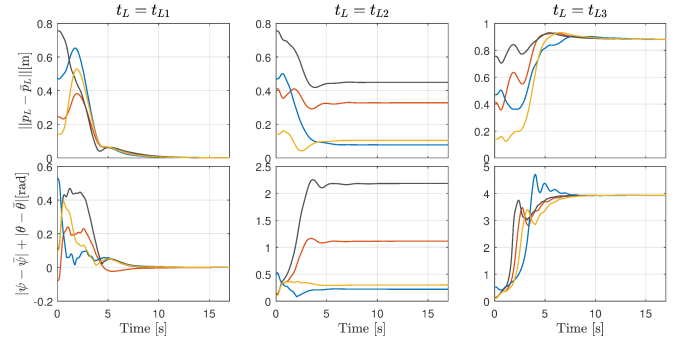


Fig. 6: Convergence to the desired load configuration for cases 1) 2) and 3). In particular the first and second rows show the position and the attitude errors, respectively, for four different initial conditions (different colors) and for the three different internal force values (columns). The attitude error is computed as the sum of pitch and yaw errors. The roll error is not considered since it is not controllable.

We observed that, as expected, for both $t_L = t_{L1}$ and $t_L = t_{L2}$ the system remains stable during the master maneuver, showing only small-amplitude damped oscillations. Once the input becomes constant, the master stops and the system converges to \bar{q} for $t_L = t_{L1}$. For $t_L = t_{L2}$, the final load attitude depends on the particular motion, and it is in general different from \bar{q} .

We tested the same motion in a more realistic case, adding Gaussian noise to the estimated state of the robots and to the measured cable force, in order to simulate real sensors. Additionally, we also considered some parameters uncertainties affecting the cables length, the load mass and the position of its center of mass. For the case 1) we can see in Fig. 7 that, even in those far from nonideal conditions, the system remains stable during the full duration of the dynamic part (until second 5), when the master moves. Once this phase is over the system converges to a stable equilibrium which is close but not equal to \bar{q} due to the imperfect knowledge of some system parameters, as expected. Simulations results for cases 2) and 3) and further simulation results are provided in the attached technical report, available at <http://homepages.laas.fr/afranchi/files/2017/TR1.zip>. Some representative simulations are available in the attached video too.

VII. CONCLUSIONS

This work deals with the cooperative manipulation of a cable-suspended load performed by two aerial vehicles. The proposed master-slave architecture exploits an admittance controller in order to coordinate the robots in a decentralized fashion but with implicit communication only, exploiting the cable forces. The passivity of the system has been proven, and the stability of the static equilibria has been studied highlighting the crucial role of the internal force. In particular, contrarily from what it is normally done in the literature (zero internal force), it is advisable to choose a positive internal force to control both position and orientation of the beam, without communication. In the future it would

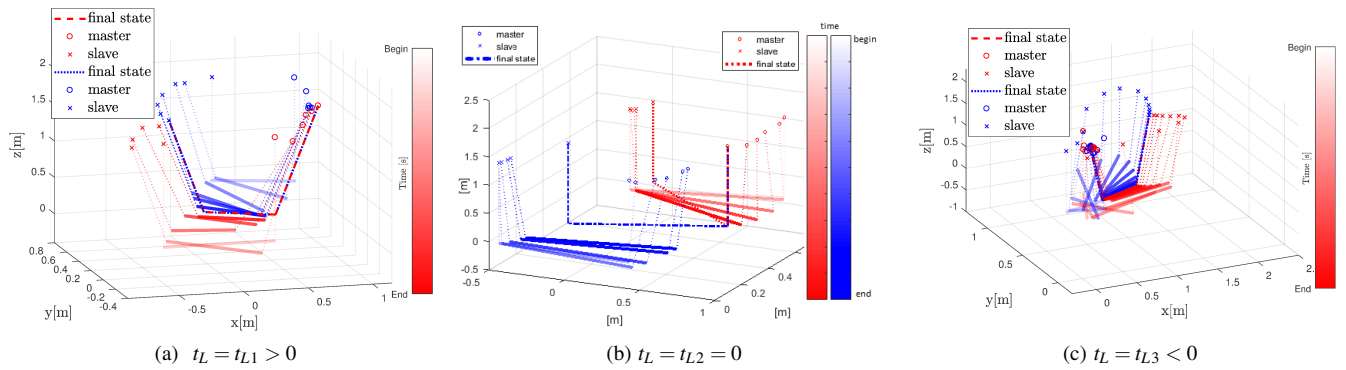


Fig. 5: Each figure shows the evolution of the system from two different initial conditions (one is shown in red and the other in blue). The two evolutions are represented as a sequence of images discriminated by the brightness of the color that represents the time (from bright/start to dark/end). The load is represented as a tick solid line, the cables as thin dashed lines, the master robot as a circle and the slave robot as a cross.

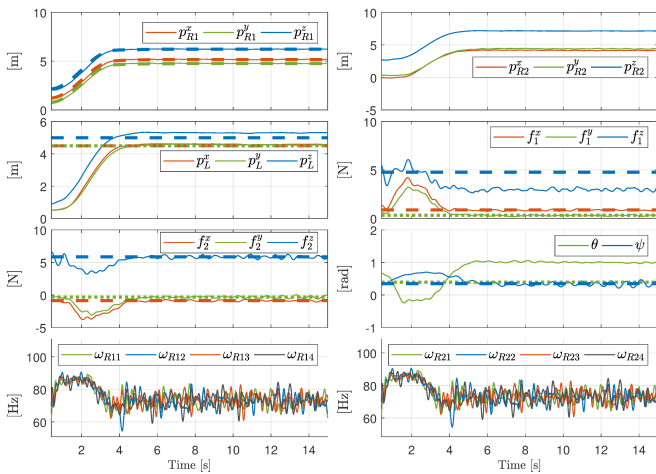


Fig. 7: Simulations results in non-ideal conditions (noisy measurements and parameter uncertainties), for a manipulation scenario, where the master is asked to follow a smooth trajectory ($\mathbf{u}_{A1}(t) \neq \mathbf{0}$). There is white gaussian noise on the position (variance 0.005 [m]) and velocity (0.01[m/s]) of the robots used in the trajectory controller and on the force (variance 0.01 [N]) that enters the admittance controllers to simulate sensors noise. The known cables rest length is 5% greater than the real one, the load mass used to generate the constant parameter π_A is 20 % greater than the real one, and the anchoring points positions in body frame have been chosen as follows: ${}^L\mathbf{b}_1 = [0.5 \ 0.01 \ 0.02][\text{m}]$, ${}^L\mathbf{b}_2 = [-0.47 \ 0.02 \ 0.03][\text{m}]$. In the plots the dashed line represents the desired value. ω_{Rij} is the angular velocity of the propeller j^{th} of the i^{th} quad-rotor.

be interesting to test the method on a real platform and to extend the analysis to a more general load. Moreover, an extension to the case of a rigid body manipulated by N robots may open the door to interesting developments.

REFERENCES

- [1] M. Tognon, B. Yüksel, G. Buondonno, and A. Franchi, “Dynamic decentralized control for protocentric aerial manipulators,” in *2017 IEEE Int. Conf. on Robotics and Automation*, Singapore, May 2017.
- [2] M. Tognon, A. Testa, E. Rossi, and A. Franchi, “Takeoff and landing on slopes via inclined hovering with a tethered aerial robot,” in *2016 IEEE/RJS Int. Conf. on Intelligent Robots and Systems*, Daejeon, South Korea, Oct. 2016, pp. 1702–1707.
- [3] M. Tognon and A. Franchi, “Dynamics, control, and estimation for aerial robots tethered by cables or bars,” *IEEE Trans. on Robotics*, vol. 33, no. 4, pp. 834–845, 2017.
- [4] I. Maza, K. Kondak, M. Bernard, and A. Ollero, “Multi-UAV cooperation and control for load transportation and deployment,” *Journal of Intelligent & Robotics Systems*, vol. 57, no. 1-4, pp. 417–449, 2010.
- [5] H.-N. Nguyen, S. Park, and D. J. Lee, “Aerial tool operation system using quadrotors as rotating thrust generators,” in *2015 IEEE/RJS Int. Conf. on Intelligent Robots and Systems*, Hamburg, Germany, Oct. 2015, pp. 1285–1291.
- [6] R. Ritz and R. D’Andrea, “Carrying a flexible payload with multiple flying vehicles,” in *2013 IEEE/RJS Int. Conf. on Intelligent Robots and Systems*, 2013, pp. 3465–3471.
- [7] F. Caccavale, G. Giglio, G. Muscio, and F. Pierri, “Cooperative impedance control for multiple uavs with a robotic arm,” in *2015 IEEE/RJS Int. Conf. on Intelligent Robots and Systems*, 2015, pp. 2366–2371.
- [8] K. Sreenath and V. Kumar, “Dynamics, control and planning for cooperative manipulation of payloads suspended by cables from multiple quadrotor robots,” in *Robotics: Science and Systems*, Berlin, Germany, June 2013.
- [9] C. Masone, H. H. Bühlhoff, and P. Stegagno, “Cooperative transportation of a payload using quadrotors: A reconfigurable cable-driven parallel robot,” in *2016 IEEE/RJS Int. Conf. on Intelligent Robots and Systems*, Oct 2016, pp. 1623–1630.
- [10] M. Manubens, D. Devaurs, L. Ros, and J. Cortés, “Motion planning for 6-D manipulation with aerial towed-cable systems,” in *2013 Robotics: Science and Systems*, Berlin, Germany, May 2013.
- [11] D. Mellinger, M. Shomin, N. Michael, and V. Kumar, “Cooperative grasping and transport using multiple quadrotors,” in *Int. Symp. on Distributed Autonomous Robotic Systems*, 2013, pp. 545–558.
- [12] Z. Wang and M. Schwager, “Force-amplifying n-robot transport system (force-ants) for cooperative planar manipulation without communication,” *The International Journal of Robotics Research*, vol. 35, no. 13, pp. 1564–1586, 2016.
- [13] A. Tagliabue, M. Kamel, S. Verling, R. Siegwart, and J. Nieto, “Collaborative object transportation using mavs via passive force control,” *arXiv preprint arXiv:1612.04915*, 2016.
- [14] M. Gassner, T. Cieslewski, and D. Scaramuzza, “Dynamic collaboration without communication: Vision-based cable-suspended load transport with two quadrotors,” in *2017 IEEE Int. Conf. on Robotics and Automation*, Singapore, 2017.
- [15] M. Ryll, G. Muscio, F. Pierri, E. Cataldi, G. Antonelli, F. Caccavale, and A. Franchi, “6D physical interaction with a fully actuated aerial robot,” in *2017 IEEE Int. Conf. on Robotics and Automation*, Singapore, May 2017.
- [16] H. K. Khalil, *Nonlinear Systems*. Prentice-Hall, New Jersey, 1996.